

OPTOELECTRONIC NEURON ARRAYS

Demetri Psaltis and Steven Lin

California Institute of Technology
Department of Electrical Engineering, 116-81
Pasadena, California 91125

The optical implementation of a neural network consists of two basic components : a 2-D array of neurons and interconnections. Each neuron is a nonlinear processing element that, in its simplest form, produces an output which is the thresholded version of the input. Liquid crystal spatial light modulators, optoelectronic integrated circuits (OEIC's), either hybrid, such as liquid crystal on silicon, Si-PLZT, and flip-chip devices, or monolithic integration in III-V compounds, are examples of such a solution. In order for these devices to be used as neurons in a practical experiment, they must contain a large number of neurons ($10^4/cm^2 - 10^6/cm^2$) and exhibit high gain. This puts a stringent requirement on the electrical power dissipation. Thus, these devices have to be operated at low enough current levels so that the power dissipation on the chip does not exceed the heat-sinking capability , and yet the current levels need to be large enough to be able to produce high gain. This means sensitive input devices are a must. To achieve these goals, the speed requirement of the devices must be relaxed as the operation of neural network does not have to be too fast.

Figure 1 shows the schematic circuit diagram of one such neuron. A metal-semiconductor field-effect transistor (MESFET) is used to drive the LED. This MESFET is in turn controlled by an input switching circuit, composed of a phototransistor, which accepts the input light, and a loading transistor. Thus, when the phototransistor detects a sufficient input light, it pulls up the loading transistor. As a result, the LED-driving MESFET is turned on and drives the LED. The advantage of this circuit design is that the LED is indirectly controlled by the the input light so that isolation between the input and the output is achieved. This enhances the sensitivity of the circuit as it can be designed such that it is switched by a very weak input light. Another feature of this neuron circuit is that the optical gain is determined by the relative output impedance of the phototransistor and the loading MESFET. Other advantage of this circuit includes the relatively mature technology in fabricating the high-gain MESFET's and a much lower electrical power dissipation required to turn on the neuron. Furthermore, the level of threshold can be adjusted on-chip by changing the gate voltage of the loading MESFET because this gate voltage will affect the amount of current the phototransistor needs to produce in order to turn on the neuron.

Figure 2 shows the device cross sectional view of the monolithically integrated optoelectronic neuron. Basically, on the semi-insulating GaAs substrate, an undoped GaAs buffer layer was first grown. Upon which, an n^+ -GaAs acting as the source and the drain ohmic contact layer on top of an n^- -GaAs current conduction channel layer were grown.

These two layers form the structure of the MESFET. On top of the n^+ -GaAs layer, a conventional double heterojunction bipolar transistor structure was grown. It consisted of an n^+ -GaAs layer as the subcollector layer, an $n\text{-Al}_{0.35}\text{Ga}_{0.65}\text{As}$ layer as the collector layer, a p-GaAs layer as the base layer, an $n\text{-Al}_{0.35}\text{Ga}_{0.65}\text{As}$ layer as the emitter layer and an n^+ -GaAs layer as the contact layer. The formation of the LED was completed by diffusing Zn twice over different areas to create the confinement for the current.

The fabrication of the optoelectronic neuron began by applying the standard degreasing and cleaning procedure to the surface of the GaAs epitaxial layers. A non-selective etch, consisting of a mixture of H_3PO_4 , H_2O_2 and CH_3COOH in the ratio of 1 : 1 : 3 was used to etch down to the n^+ -GaAs layer to define the LED and the phototransistor. After which, the same etch was used to etch down the semi-insulating substrate to define the MESFET. A blank deposition of Si_3N_4 was then applied to the surface of the device by using a thermal chemical vapor deposition system heated to 610° . The gases used were silane diluted to 1% by nitrogen, ammonia and nitrogen. A thickness of approximately 1200 Å to 1500 Å of Si_3N_4 , which exhibited a color of blue to light blue, was deposited. The next step was Zn-diffusion to convert the $n\text{-AlGaAs}$ emitter layer to p-AlGaAs for the upper cladding layer for the LED as well as to provide the current confinement. This was achieved by selectively removing the Si_3N_4 over the the LED window area in a CF_4 plasma and performing a sealed ampoule Zn-diffusion process. The ampoule, in which the neuron device and the diffusion source, ZnAs_2 were placed, was pumped to a vacuum of 8×10^{-8} torr before it was sealed with a torch. The ampoule was then inserted into a furnace of 640° to promote the diffusion of Zn into the exposed area of the LED for approximately 9 minutes. Afterwards, the ampoule was quickly quenched. Usually there was As condensation on the inner wall of the ampoule after quenching to indicate the proper diffusion of Zn into the LED. A second diffusion process was carried out by using exactly the same procedure except the diffusion time was approximately 5 minutes and the area of diffusion was slightly larger. After the Zn-diffusion step, selective area of Si_3N_4 was again removed in CF_4 plasma to facilitate the subsequent ohmic contacts for the source and the drain as well as the gate recessed area of the MESFET, and the contacts for the emitter and the collector of the phototransistor. The transistor contact terminals, including the source and the drain, and the emitter and the collector of the phototransistor, were metalized by evaporating AuGe/Ni/Au of 200 Å, 100 Å, and 1500 Å, respectively, by using the lift-off technique and subsequently alloyed at 430°C in an N_2 ambient for 4 minutes to drive in the Ge in forming the ohmic contacts. The gate recess etching process was then performed by monitoring the source-drain current in the MESFET. This etching used the Si_3N_4 as the mask in order to obtain a self-aligned recess. The etching was stopped when the desired source-drain saturation was obtained. The etchants used in recessing the gate was NH_4OH , H_2O_2 and H_2O in a ratio of 20, 7 and 973 respectively. The etch rate was approximately 30 Å/second. Next, the gate was defined by evaporating first 150 Å of Ti and then 1500 Å of Au by an electron beam evaporator. The excess metals were lifted off in acetone. The area of the gate was $6 \times 100 \mu\text{m}^2$ and was self-aligned asymmetrically to the edge of the source inside the recessed region. The last step was to remove the light-absorbing n^+ -GaAs cap layer in the phototransistor by wet etching. The entire processing of the optoelectronic neuron utilized 9 masks. Figure 3 shows the photograph of a complete neuron. The entire

area, including the contact pads, measured approximately $400 \times 400 \mu\text{m}^2$. However, the active device area was only about $150 \times 250 \mu\text{m}^2$.

The neuron was tested by illuminating the phototransistor window area by a GaAs laser diode. This was achieved by splitting the output beam of the laser diode by a beam splitter into 2 equal-intensity beams. One of the beams was focused onto the phototransistor and the other beam was focused into the detector in order to monitor the power of the beam incident on the phototransistor. The overall input-output characteristics of the optoelectronic neuron was obtained by monitoring the output power from the LED as a function of the laser input power incident on the phototransistor at a fixed gate voltage on the loading MESFET. Figure 4 shows the two of these plots. One of them was taken at a gate voltage of -3.0 V and the other one was taken at a gate voltage of -2.4 V. For the curve with a gate voltage of -3.0 V, the output remained zero until the input power reached approximately $3 \mu\text{W}$. Beyond this point, the output power increased rapidly to $12 - 15 \mu\text{W}$ over an additional input of $2 \mu\text{W}$. This represented a differential optical gain of 6. The threshold of the neuron was controlled by applying a different voltage to the gate of the loading MESFET, as clearly seen in the plot. Because of the leakage in both the loading MESFET and the output driving MESFET, a minimum $3 \mu\text{W}$ was necessary to turn on the neuron. By reducing the leakage currents through the gate in both MESFET's, this number is expected to drop substantially. During the on-state of the neuron, the LED current was measured to be 1.2 mA. This implied an electrical power dissipation of 2.4 mW by using a 2-volt power supply on the the output driving circuit. When the input laser beam was pulsed to a level just enough to turn on the neuron, the output LED current showed a rise time of $5 \mu\text{sec}$. This meant that the neuron could be turned on with an optical switching power of only $(2 \mu\text{W}) \times (5 \mu\text{sec}) = 10 \text{ pJ}$ [1]. Thus, this optoelectronic neuron exhibited comparable switching energy as compared to the SEED devices [2].

The differential optical gain of 6 was limited by the finite output impedance of the phototransistor and the loading MESFET as well as the leakage currents in the MESFET's. The output impedance of the phototransistor could be increased by doping the base more heavily. However, this reduced the current gain of the phototransistor. As a result, the base thickness had to be reduced to compensate for the increased doping concentration in order to maintain the same current gain. Unfortunately, reducing the thickness the base layer adversely affected the absorption efficiency of the phototransistor. Therefore, an optimized design had to be used. The output impedance of the loading MESFET could be increased by using a more insulating substrate as well as reducing the leakage current through the gate. It was interesting to note that reducing leakage current has a lot of benefits in term of improving the optical gain and the sensitivity of the neuron. Thus, the same optoelectronic neuron was fabricated again by carefully cleaning the surface before the gate metalization was defined. Furthermore, a different gate metalization composition was employed. This was consisted of the same Ti/Au metals except an 100-Å layer of Pt was inserted between the Ti and the Au. The doping concentration of the MESFET conduction layer was also reduced to $5 \times 10^{16} \text{ cm}^{-3}$ for less leakage current across the gate. Figures 5 [3] shows the improved results of the neuron, which incorporated the above-mentioned simple changes.

The testing conditions were the same as before except the gate of the loading MESFET

was floating. This was intended to reduce the gate-drain leakage current furthermore. It is evident from the plot that, by reducing the gate-drain leakage current, the minimum input power needed to turn on the neuron was reduced. In this case, the input power was measured to be $1 \mu\text{W}$. Moreover, the differential optical gain also increased dramatically to 40 as an additional input power of $0.2 \mu\text{W}$ beyond the threshold caused a change of $8 \mu\text{W}$ at the output. This improvement was remarkable considering the only improvement made was to reduce the gate leakage current of the loading MESFET. Not only was the differential optical gain improved, the absolute optical gain had increased to 8. The current drawn by the LED during the on-state of the neuron was measured to be 0.8 mA . Therefore, the electrical power dissipation per neuron was 1.6 mW by using a 2-volt power supply. The speed of the neuron was also measured by applying an electrical pulse to the laser diode that illuminated the phototransistor. A rise time of $65 \mu\text{sec}$ was obtained in this neuron. This implied a total optical switching energy of $(65 \mu\text{sec} \times 0.2 \mu\text{W}) = 13 \text{ pJ}$. This optical switching energy was comparable to that of the previous neuron, which was 10 pJ . This is expected because the total charges needed to charge up the gate of the output driving MESFET's, which had the same gate width and length, in both neurons were the same. Since the voltage swings at the same gate from the off-state to the on-state of the neuron were also the same, the switching energy, which was equal to QV , remained unchanged. Thus, overall, the neuron became more sensitive and provided more gain. However, this was achieved at the expense of a lower switching speed.

Another factor that limited the performance of the optoelectronic neurons was the efficiency of the detector, which, in this case, was the double-heterojunction bipolar phototransistor. Because of the relatively thick base layer, the current gain, β , of the phototransistor was low. Since the overall goal of the neuron was to achieve a high-gain optical thresholding device at as low input power level as possible, high-efficiency or even high-gain detectors at low input power level was vital to the success of the neuron. For this reason, optical FET's were developed. The operational principle of an optical FET was similar to that of a conventional MESFET except the gate metalization was not physically defined to allow for the external illumination to be absorbed in this area. In addition to the inherent high optical gain achievable in the optical FET, the structure of the optical FET was identical to that of the MESFET. This meant that optical FET's could be easily implemented into the existing material and process. This was a very important advantage of having the optical FET.

This neuron was tested at the same conditions as the previous one. Again, the gate of the loading MESFET in the input switching stage was left floating to minimize the gate leakage current. The optical input-output characteristics are shown in Fig. 6. Because of the insufficient recess in the gate of the output driving MESFET, this MESFET was not pinched off at zero gate bias. As a result, a current flowed between the source and the drain with zero input power onto the optical FET. This caused a non-zero LED output power at zero input power level. The remedy to this problem was to recess the gate of the LED-driving MESFET further until the current was close to zero at zero gate bias. This would shift the entire input-output curve shown in Fig. 6 down to the origin so that a normal neuron input-output characteristics could be obtained. Despite the gate recess problem, the differential optical gain measured was quite impressive. The output rose by

4.3 μ W over an input swing of 54 nW. This corresponded to a differential optical gain of 80 [4]. It is also worth noting that the minimum input power needed to turn on the neuron had dropped significantly from the previous 1 μ W down to about 5 nW. This could be attributed to the higher efficiency of the detector as well the overall reduction in the gate leakage current. Since this initial thresholding power was very small, the absolute optical gain was approximately the same the differential optical gain assuming the gate of the output MESFET was properly recessed. During the on-state of the neuron, the total current drawn by the LED was 0.9 mA, which implied an electrical power dissipation of 1.8 mW/neuron. Again, if the gate were properly recessed, this dissipation power would be reduced by 50%. A rise time of 700 μ sec was measured. When this was multiplied by the optical switching power of 54 nW, an optical switching energy of 38 pJ was obtained. Again, this was on the same order of magnitude as the previous optical switching energies. This indicated that the speed of the neuron was limited by the charging process of the gate capacitance and varied inversely proportional with the input power level. Table 1 summarizes the results of the optoelectronic presented in this paper.

	Phototransistor-based neuron	Phototransistor-based neuron with gate leakage reduction	Optical FET-based neuron
OUTPUT POWER	12 μ W	8 μ W	9 μ W
DIFFERENTIAL OPTICAL GAIN	6	40	80
ABSOLUTE OPTICAL GAIN	2.5	8	150
RISE TIME	5 μ sec	65 μ sec	700 μ sec
SWITCHING POWER	2 μ W	0.2 μ W	54 nW
MINIMUM THRESHOLD	3 μ W	1 μ W	5 nW
OPTICAL SWITCHING ENERGY	10 pJ	13 pJ	38 pJ
ELECTRICAL POWER DISSIPATION	2.4 mW	1.6 mW	1.8 mW

Table 1 Summary of the neuron characteristics for three versions of optoelectronic neurons discussed in this paper.

In summary, the performance of the optoelectronic neuron is expected to achieve a level that makes possible a dense integration of these devices in a large array form in the

near future. Specifically, an optical gain on the order of 100, which is not far from the present demonstrated gain of 80, should be easily obtained. Electrical power dissipation on the order of $100 \mu\text{W}$ per neuron should be achievable if the detector sensitivity is increased and the leakage current in the circuit is decreased. This allows the operating current in the neuron to be lowered without sacrificing the optical gain. With $100 \mu\text{W}$ power dissipation per neuron, an 100×100 array of optoelectronic neurons can be inserted into an optical system in which practical optical interconnects are demonstrated with holograms without being limited by the heat sinking capability of the chip. Finally, along with the increase in the input detector sensitivity, the optical switching power is expected to decrease proportionally. With further optimization in minimizing the gate capacitance of the transistor, the overall optical switching energy is also expected to decrease. At that state, the limiting factor in expanding the size of the array will not be the heat dissipation issue, but rather and most likely the photolithography capability.

Acknowledgment

This work is supported by DARPA. S. Lin has been supported in part by a fellowship from the Jet Propulsion Laboratory.

Reference

- [1] S. H. Lin, F. Ho, J. H. Kim, and D. Psaltis, "GaAs-Based Optoelectronic Neurons", Technical Digest of Optical Computing Conference, Salt Lake City, UT, March 4-6, pp. 295, 1991.
- [2] A. L. Lentine, H. S. Hinton, D. A. B. Miller, J. E. Henry, J. E. Cunningham, and L. M. F. Chirovsky, "Symmetric Self-Electrooptic Effect Device : Optical Set-Reset Latch, Differential Logic Gate, and Differential Modulator/Detector", IEEE J. Quantum Electron., Vol. QE-25, pp. 1928, 1989.
- [3] S. H. Lin, F. Ho, J. H. Kim, and D. Psaltis, "Monolithic Integrated Optoelectronic Thresholding Devices for Neural Network Applications", Technical Digest of Conference on Lasers and Electro-Optics, Baltimore, MD, May 12-17, pp. 82, 1991.
- [4] S. H. Lin, D. Psaltis, and J. H. Kim, "High-Gain GaAs Optoelectronic Thresholding Devices for Optical Neural Network Applications", Technical Digest of Integrated Photonic Research Conference, Monterey, CA, April 9-11, pp.8, 1991.

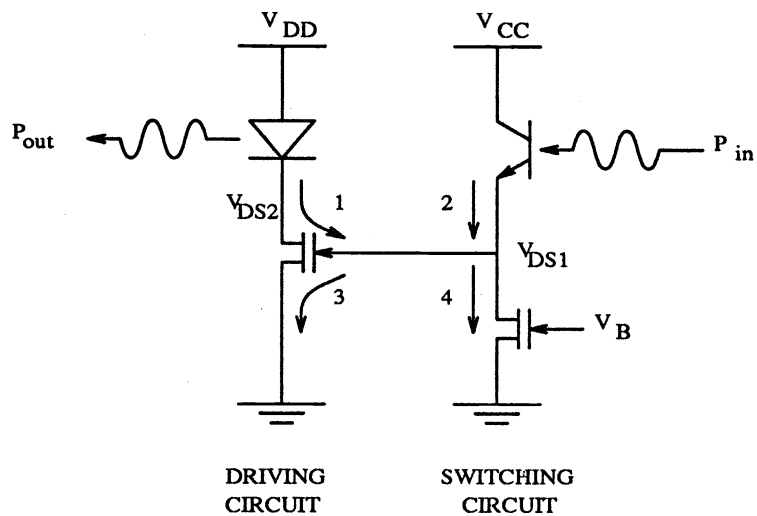


Fig. 1 Schematic circuit diagram of the optoelectronic neuron that incorporates two MES-FET's, a phototransistor and a LED.

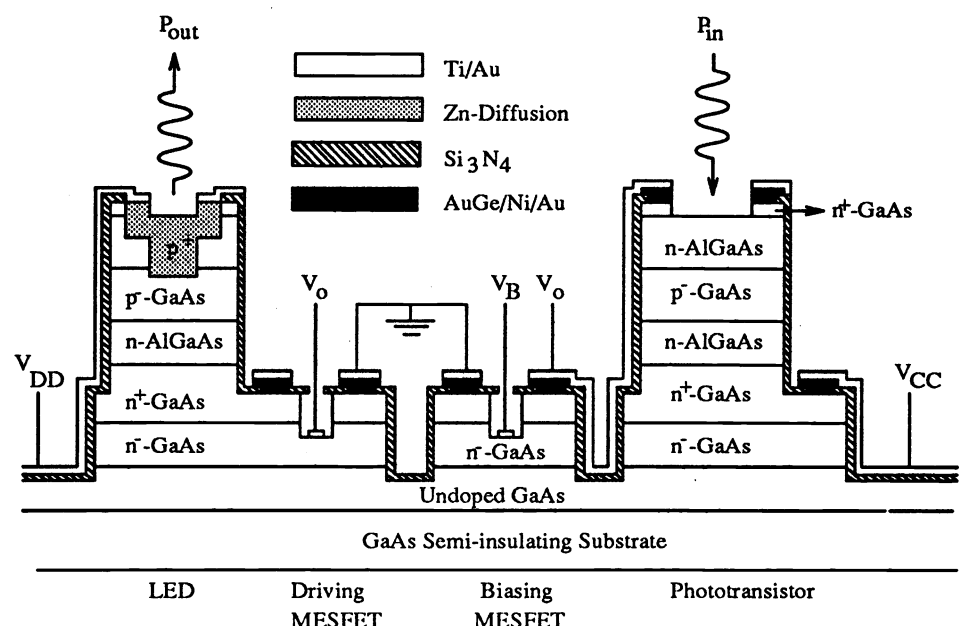


Fig. 2 The cross sectional view of the optoelectronic neuron monolithically integrating 2 MESFET's, a LED and a phototransistor.

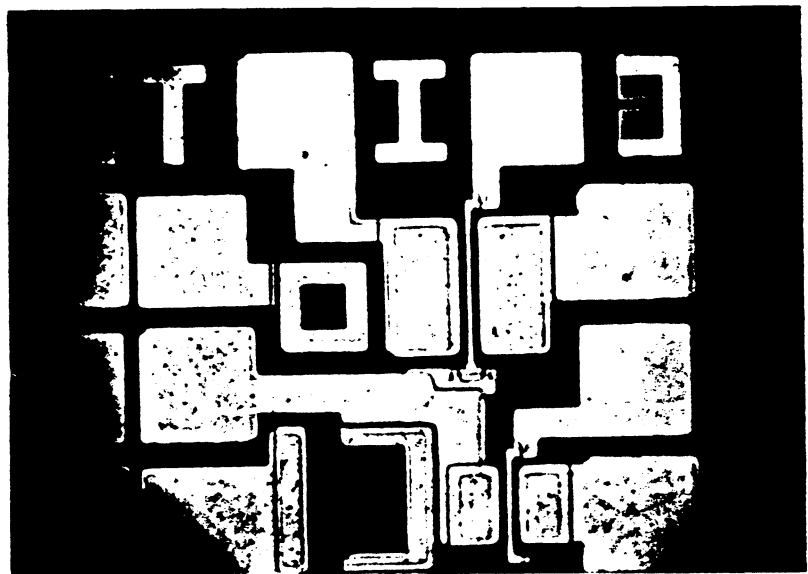


Fig. 3 Photomicrograph of a completely fabricated optoelectronic neuron.

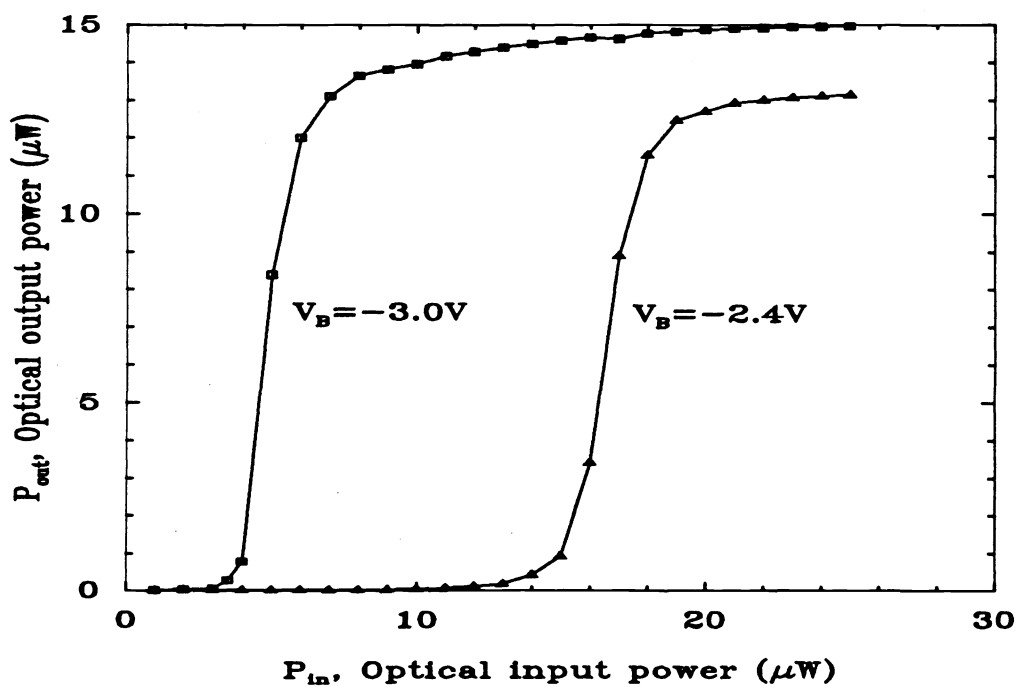


Fig. 4 Input-output characteristics of the optoelectronic neuron incorporating a phototransistor as the detector. V_B is the bias voltage on the gate of the input switching circuit.

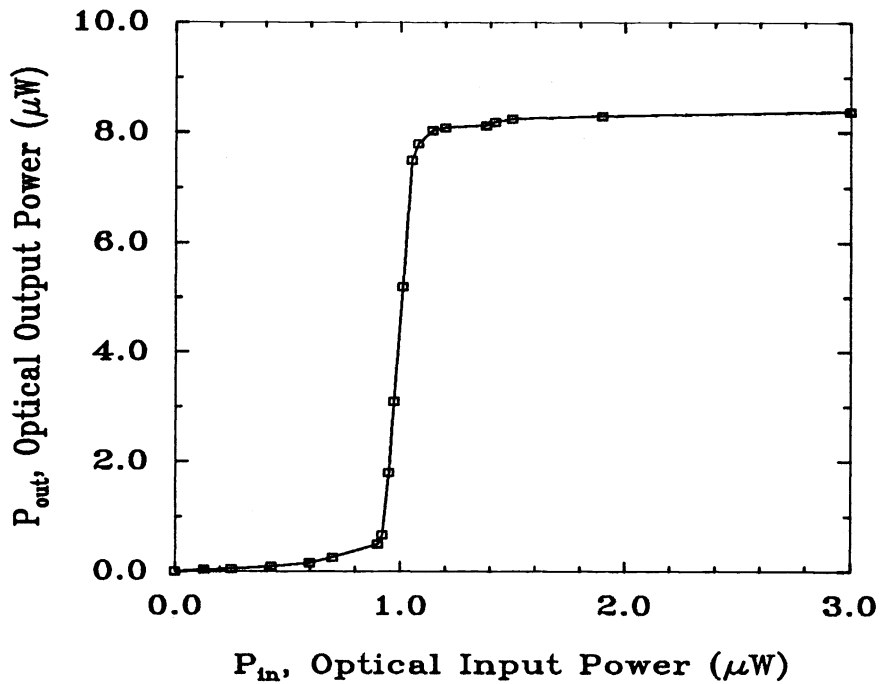


Fig. 5 Input-output characteristics of the improved optoelectronic neuron, showing a differential optical gain of 40 and an absolute optical gain of 8.

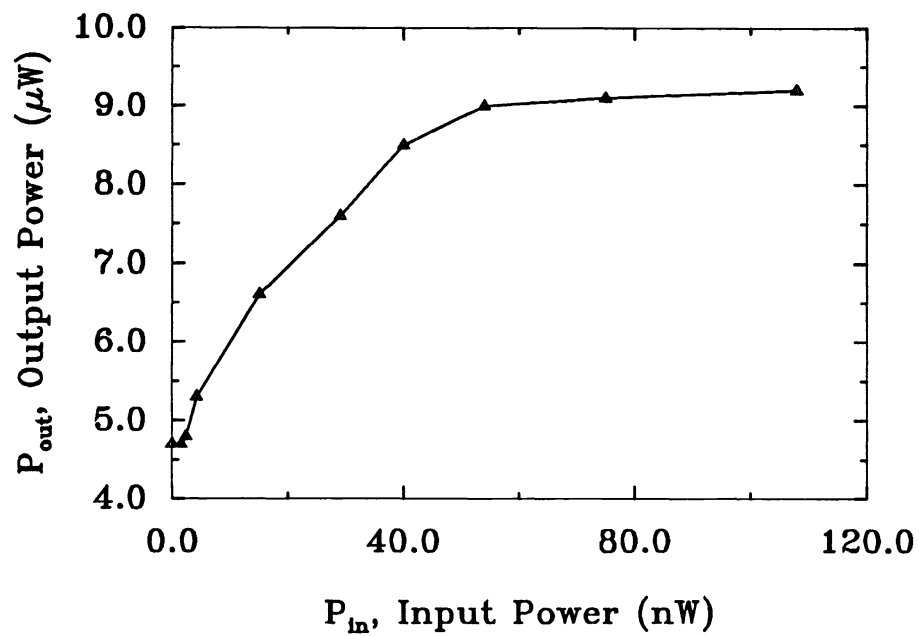


Fig. 6 Input-output characteristics of the optical FET-based optoelectronic neuron. A differential optical gain of 80 was measured in this neuron.